ACES Asian Chemical Editorial Society

DOI: 10.1002/asia.201900385

CHEMISTRY AN ASIAN JOURNAL Full Paper

SPECIAL ISSUE

Motion of Enzyme-Powered Microshell Motors

Chengtao Chen,[a] Zhengqing He,[b] Jie Wu,*[a] Xueqing Zhang,[a] Qianfeng Xia,[b] and Huangxian Ju*[a]

Abstract: Microshells are attractive in constructing bubble-propelled micromotors due to the lower energy consumption for bubbles forming on a concave surface. In this work, enzyme-powered microshell motors were fabricated on multimetallic (Au/Ag/Au) microshells along with the modification of catalase on its concave surface. The catalase triggered the decomposition of hydrogen peroxide to oxygen gas, hence propelling the autonomous motion of microshell motors. A size-dependent motion behaviour was observed for the microshell motors in the form of slow tremble and fast translation motion for a size smaller and larger than 5 μm, respectively, according to the size, generation efficiency and ejection mechanism of bubbles and the intensity of Brownian motion. In addition, the effect of fuel concentration on the motion speed of microshells was dependent on whether the bubble generation was affected by the limited mass transfer in the microshell space. These findings play an important role for the design of microshell motors.

Introduction

Because micromotors can perform motion in different environments by converting energies, for example optical,[1] magnetic,[2] electrical,[3] ultrasonic,[4] chemical[5] and biological[6] energies, into mechanical and kinetic energy, they have attracted great attentions in multiple fields. For specific demand in application, multifarious micromotors such as microrods,[7] microtubes,[8] Janus microspheres[9] and other irregular shapes[10] have been created by diverse methods. Due to the ability of auto propulsion and convenient direction control, micromotors possess advantages of self-separation, active recognition, and accelerating mass transfer, hence showing charming performance in environmental remediation,[11] biosensing,[12] clinical diagnosis,[13] drug delivery[14] and therapy.[15]

Catalytic micromotors containing on-board catalyst are one kind of important motors because they can realize self-driving only by harvesting chemical energy from the surrounding fuel environment without external stimuli. Among them, bubble propelled micromotors are most widely studied due to their fast speed and superior efficiency.[16] Bubble propelled micromotors are driven through the detachment or bursting of bubbles produced by special catalytic combinations, for example Pt/H_2O_2. Platinum based tubular motors and spherical Janus motors are two kinds of well-developed bubble propelled micromotors, in which the former is characterized by quick motion due to the intracavity concave structure of catalytic layer,[17] and the latter is characterized by easy modification on the catalytic layer in the outermost shell.[18] Recently, enzyme powered catalytic micromotors were fabricated owing to their good biocompatibility for biological applications.[19]

Microshells benefitted from their unconfined concave structure are good candidates for fabrication of bubble-propelled micromotors. Usually, bubble-propelled microshell motors are multimetallic shells with Pt concave layer.[20] Based on the catalytic decomposition of hydrogen peroxide by Pt, these microshell motors could be propelled by O_2 with quick motion speed ever without chemical asymmetry. This is because the concave catalytic layer in microshell requires less energy for bubbles forming than flat and convex surface.[21] In addition, the microshells could form local microspace on concave surface in which O_2 can reach saturation easily for bubble ejection. However, the research of microshell motors is mainly on the fabrication of platinum based microshells with size of tens of micrometers, microshells at size of few or sub-micrometers, especially microshell motors fabricated with molecular catalyst, are rarely reported.

Herein, enzyme powered microshells with different sizes were prepared and their motion behaviours were systematically studied. The micromotors were fabricated on multimetallic (Au/Ag/Au) microshells in which catalase was modified on its concave surface to catalytically produce oxygen and drive motors. The results showed the enzyme-powered microshells were propelled by bubble generation, regardless of the size, however, their motion behaviour was size-dependent relying on the bubble size, generation efficiency and ejection way, as well as their Brownian motion intensity. The effect of fuel concentration on motion speed of microshells with different sizes

[a] C. Chen, Dr. J. Wu, X. Zhang, Prof. H. Ju
State Key Laboratory of Analytical Chemistry for Life Science
School of Chemistry and Chemical Engineering
Nanjing University
163 xianlin Road, Nanjing 210023 (P. R. China)
E-mail: wujie@nju.edu.cn
hxju@nju.edu.cn

[b] Z. He, Prof. Q. Xia
Laboratory of Tropical Biomedicine and Biotechnology
School of Tropical Medicine and Laboratory Medicine
Hainan Medical University
Haikou, 571199 (P. R. China)

Supporting information and the ORCID identification number(s) for the author(s) of this article can be found under: https://doi.org/10.1002/asia.201900385.

This manuscript is part of a special issue on Smart Chemistry, Smart Motors. Click here to see the Table of Contents of the special issue.

was different. Bienzyme (Glucose oxidase (GOx) and Catalase) powered microshell motors were further fabricated and their driving in glucose followed the size-dependent motion mechanism.

Results and Discussion

Preparation and Characterization of Microshells.

A template-directed deposition protocol was employed to prepare microshells with different size.[22] Briefly, SiO_2 microspheres at different size were spread onto glass substrates to form monolayer, then Au, Ag, Au were sputtered onto the template successively. After the dissolution of SiO_2 template in etching solvent, microshells were prepared. Here, Au/Ag/Au microshells were adopted to fabricate micromotors owning to the ability of silver alloy accelerated catalytic decomposition of H_2O_2.[23] The thickness of metal layers varied with the size of microshell to assure the shells with stable structure and smallest weight. In this work, the thickness of Au/Ag/Au was optimized to 50/200/50 nm, 30/120/30 nm, 20/80/20 nm, 10/40/10 nm, and 4/16/4 nm for preparation of microshells at 20 μm, 10 μm, 5 μm, 2 μm, and 1 μm and 500 nm, respectively.

The SEM images of microshells from 2 to 20 μm were shown in Figure 1. All the prepared Au/Ag/Au microshells showed a mechanical stable hemispherical structure. Both the concave and convex surface of the microshells were regular, smooth and compact, which was in favor of further modification. In addition, the half spherical structure of the microshells offered a local semi-enclosed microspace surrounded by concave surface, benefitting the generation of bubbles.

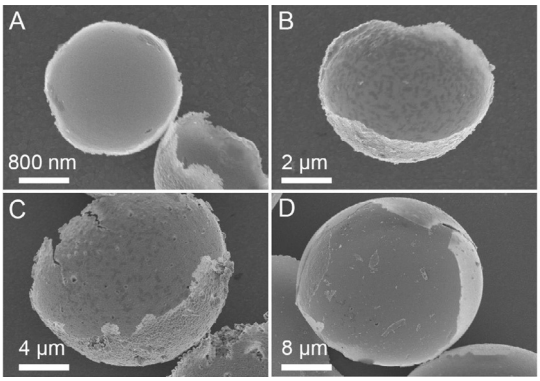

Figure 1. SEM images of microshells at (A) 2, (B) 5, (C) 10, and (D) 20 μm.

Motion of Catalase Powered Microshell Motors.

By asymmetric modification of catalase on the concave surface of microshells, the enzyme powered microshell motors were fabricated, in which 11-mercaptoundecanoic acid (MUA) and 6-mercapto-1-hexanol (MCH) were assembled on concave and convexrespectively to offer chemical activity and inert surface for catalase binding. The motion of microshell motors in 500 mM H_2O_2 was observed (Figure 2 and Video S1). The trajectories showed the motion behavior of micromotors varied with the sizes of microshells. For 2 μm microshell motors, bubble was invisible and a tremble behaviour was observed (Figure 2 A). In contrast, visible bubbles were appeared on microshells at 5, 10 and 20 μm, and the efficiency of bubble generation as well as the amount of motion-active microshells were increased with increasing the size (Figure 2 B, C and D). However, bubble propelled translation motion was observed on microshells at 10 and 20 μm rather than 5 μm. Obviously, the motion behaviour of microshell motors depended on both the bubble generation and the shell weight. Due to the small superficial area as well as the small openings size of 2 μm microshells, a little amount of catalase would be modified on the concave to produce O_2, hence, bubbles with small size and low generation efficiency were produced, resulting in a weak driving force. Owing to the small size and weight, Brownian motion was obvious for 2 μm microshells, and the weak driving force could only enhance the Brownian motion to perform intense tremble. For microshells at 5, 10 and 20 μm, Brownian motion was not obvious and could be neglected, thus, their motion completely relied on the gas driving force. Similar to 2 μm microshell, 5 μm microshell also produced weak driving force because of the low generation efficiency, but it had relatively heavy body, thus, 5 μm microshells were stationary in the fuel solution. As the size bigger than 10 μm, large amount of enzymes could be modified on concave due to the large superficial area as well as the big openings size of microshells, hence, bubbles with big size and high generation efficiency was produced to occur strong propelling force. Thus, a directional translation motion with quick speed was observed for microshell motors at 10 and 20 μm. Besides, the motion trajectory of these large size microshells was determinative to be circular or straight according to the velocity and force/torque produced by the micromotors.[24] Here, most microshells presented circular trajectory, and the straight motion was observed only for low speed microshells. In addition, the motion

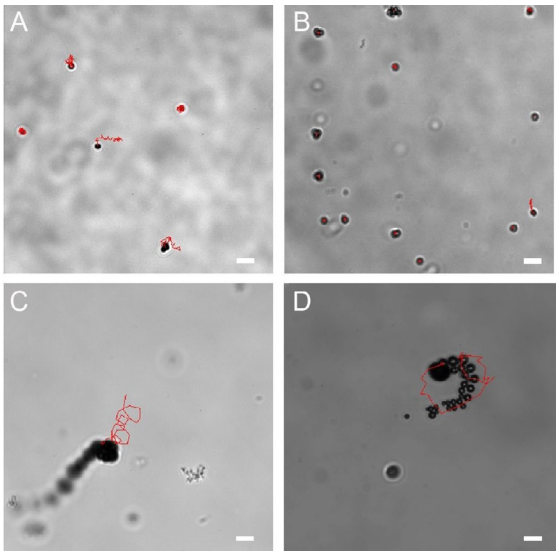

Figure 2. Motion trajectories of catalase powered microshell motors at size of (A) 2, (B) 5, (C) 10 and (D) 20 μm during a period of 3 s. Scale bar: 10 μm.

speed of the micromotors was size-dependent due to the bubble generation efficiency, thus, 20 μm microshells presented a faster motion speed than 10 μm microshells. The result was consistent with that of platinum based microshell motors reported previously.[21,25]

The bubble generation on 2 μm microshells was observed by microscope. For image recording, the microshells were immobilized on the glass slide with their opening upward. In contrast to microshells soaked in water, periodic change of the brightness in microshell space was observed after the microshells were soaked in 100 mM H_2O_2 (Video S2), suggesting the generation and burst of microbubbles. This phenomenon was further confirmed by the intensity curve (Figure 3). Compared

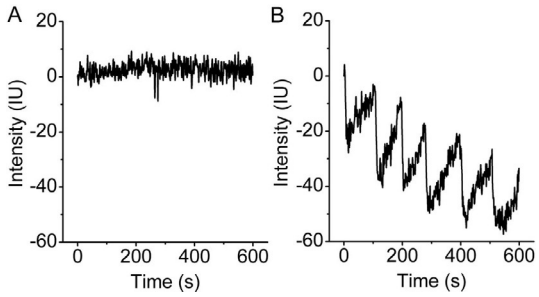

Figure 3. Intensity curves of 2 μm microshells soaked in (A) water and (B) 100 mM H_2O_2 during a period of 10 min.

with the background curve showing constant intensity in water, a curve with periodic triangular pulse change of the intensity was observed in H_2O_2. The gradual increase and sharp reduction of the intensity were attributed to the growth and burst of the microbubbles, respectively,[26] verifying the periodic generation and burst of microbubbles on 2 μm microshells. In addition, the intensity was changed with a regular frequency of 100 ± 11 s (Figure 3B), indicating the generation of a bubble on 2 μm microshells required ≈100 s. Such low bubble generation efficiency resulted in a weak driving force, hence the low speed tremble behaviour of 2 μm microshells.

The bubble enhanced tremble of 2 μm microshells was also characterized by optical microscopy (Video S3). Automatic tracking showed the microshells travelled longer trajectories in 100 mM H_2O_2 than that in water, and the mean velocity of ten microshells in the fuel solution was 20 μm s^{-1}, which was obviously faster than 7 μm s^{-1} of Brownian motion in water, indicating the occurrence of bubble enhanced tremble for 2 μm microshells (Figure 4A and B). The mean-square-displacement (MSD) at different time interval (Δt) of 2 μm microshell was calculated (Figure 4C). Compared with that in water, the MSD curve obtained from fuel solution showed the corresponding parabolic shape at short time, further confirming the performance of bubble enhanced tremble rather than Brownian motion of 2 μm microshells in H_2O_2.

The above experiments indicated the catalase powered microshell motors were propelled by bubble, regardless of the size, however, their motion speed and behaviour were size-dependent due to the size, generation efficiency and ejection way of bubbles. The motion mechanism of the microshells with different size was presented in Scheme 1 and Video S4. For microshells with size lower than 5 μm, bubbles at few micrometer or sub-micrometers were generated slowly and burst instantly in the microshell space. The energy of bubble collapse formed the driving force of microshells,[27] however, due to the low generation frequency, the bubble driving force was weak and could only propel the microshells slightly. By combining the weak bubble driving motion with the Brownian motion, the microshells with small size would follow the behaviour of tremble with low speed. On the other hand, for microshells with size bigger than 5 μm, a large number of visible bubbles were generated rapidly on the concave surface of the microshells, resulting in the quick saturation of O_2 and the immediate detachment of bubbles from the shell without bursting. The high efficiency of bubble generation and ejection produced a strong driving force which made the microshells with big size follow the behaviour of translation motion with quick speed.

Effect of Fuel Concentration on the Motion of Microshells.

The motion of microshells at different size in H_2O_2 with different concentrations was observed (Figure 5). For 20 μm microshells, motion was observed only when H_2O_2 was higher than 100 mM, and their velocity was increased sharply with increasing the H_2O_2 concentration and reached the maximum speed ≈180 μm s^{-1} at 1000 mM H_2O_2. One thing to be noted, because the bubble size and generation frequency were correlated negatively and positively with H_2O_2 concentration, these microshells were driven by bubble burst and ejection in 100 and 1000 mM H_2O_2, respectively. In contrast, for 2 μm microshells, tremble was always observed no matter the H_2O_2 concentra-

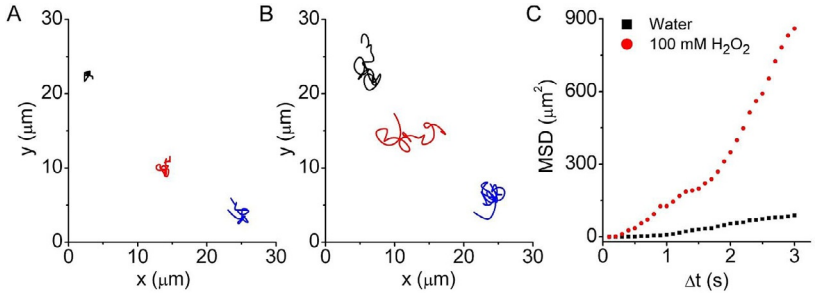

Figure 4. Trajectories of three 2 μm microshells in (A) water and (B) 100 mM H_2O_2 during a period of 3 s. (C) Average MSD as a function of time interval (Δt).

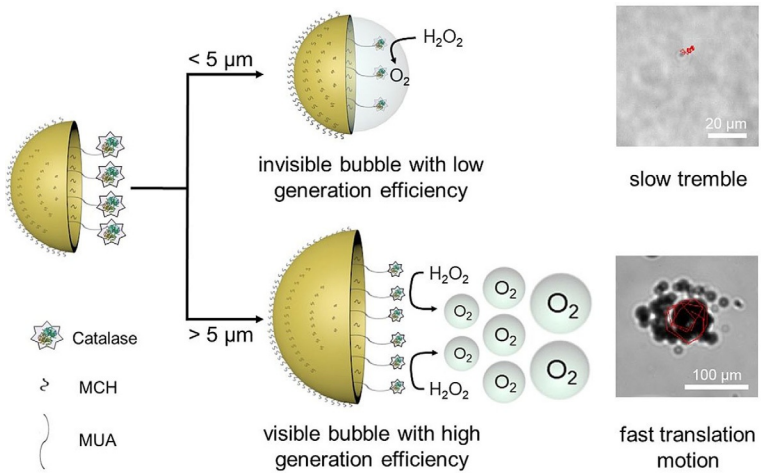

Scheme 1. Motion mechanism of catalase powered microshell motors.

tion due to the Brownian motion. Their velocity was slowly increased to reach the maximum $\approx 20\ \mu m\ s^{-1}$ at 100 mM H_2O_2, and the microshells maintained this maximum speed when H_2O_2 concentration was higher than 100 mM (Figure 5A). Similar trend of velocity vs. H_2O_2 concentration as well as maximum speed was observed for microshells at 500 nm and 1 μm, except that the fuel concentration required to reach the maximum speed was different (Figure 5B and C). The plateau appeared at 1 and 10 mM H_2O_2 for 500 nm and 1 μm microshells, respectively. The dependence of velocity on H_2O_2 concentration confirmed all size of microshells follow the bubble propelled motion mechanism. In addition, these results indicated the influence of fuel concentration on large size microshells was greater than that on small size microshells. This should be because, for large size microshells who performed translation motion, H_2O_2 concentration was the determinant of bubble generation, however, for small size microshells who performed tremble, the sub-micro shell space limited the molecular mass transfer, which restricted the bubble generation for motion propulsion.

Bienzyme Powered Microshell Motors.

Following the fabrication procedure of catalase modified microshells, catalase and GOx in a certain proportion were modified on the concave surface of microshells to construct bienzyme powered microshell motors. Here, GOx catalysed glucose to produce H_2O_2 which then immediately decomposed by catalase to generate oxygen bubbles for motion propulsion of the microshell motors (Figure 6A). The catalase-GOx microshells at 20 μm were motionless in glucose solution at any concentration, however, the bienzyme microshells at 2 μm exhibited obvious tremble motion in fuel solution (Video S5). The longer trajectory and parabolic shaped MSD curve obtained from the 100 mM glucose indicated the bienzyme microshells at small size could perform the bubble enhanced tremble similar to the catalase modified microshells (Figure 6B, C, and D). In addition, the dependence of velocity on glucose concentration also verified the bienzyme microshells at small size carry on the bubble propelled motion mechanism (Figure 6E). For catalase-GOx microshells, a small amount of H_2O_2 was produced by the catalytic reaction of GOx to glucose, thus, 2 μm rather than 20 μm bienzyme microshells exhibited obvious motion behaviour because the 2 μm microshells were less dependent on fuel concentration than the 20 μm microshells which was concluded in catalase modified microshells above.

Conclusions

This work studied the motion behaviours of enzyme-powered microshell motors with different sizes. Bubble propulsion occurred on catalase-modified microshells, regardless of the size, but the motion behaviour of microshell motors was size-dependent according to the bubble size, generation efficiency and ejection way, as well as the shell weight. Microshells with a size smaller than 5 μm exhibited a slow tremble behaviour due to the weak driving force from the burst of invisible bubble with a slow generation frequency. In contrast, microshells with a size larger than 5 μm exhibited a fast translation motion by the strong driving force from the quick detachment of visible bubbles with high generation efficiency. In addition, the influence of fuel concentration on large size microshells was greater than that on small size microshells because the bubble generation was restricted by the limited mass transfer in the microshell space of the latter. Furthermore, catalase-GOx powered bienzyme motors could be fabricated on microshells with a size of 2 μm rather than 20 μm, and also exhibited a

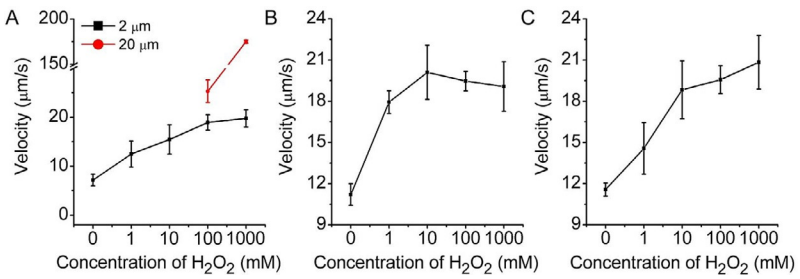

Figure 5. Effect of the concentration of H_2O_2 on the motion velocity of microshells at size of (A) 2 and 20 μm, (B) 500 nm, and (C) 1 μm.

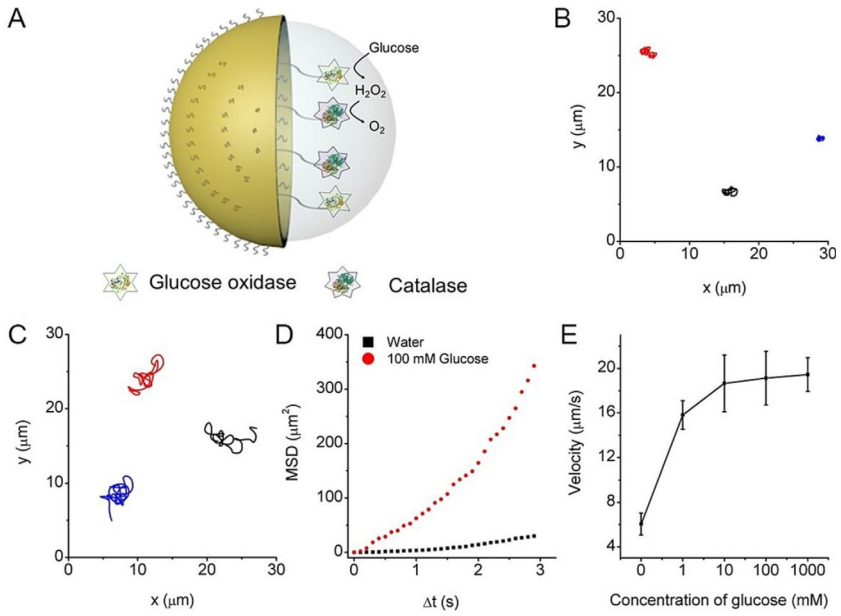

Figure 6. (A) Schematic motion of catalase-GOx powered microshell motors. Trajectories for three 2 μm catalase-GOx modified microshells in (B) water and (C) 100 mM glucose during a period of 3 s. (D) Average MSD as a function of time interval (Δt). (E) Effect of glucose concentration on motion velocity.

bubble-propelled tremble behaviour. These findings could guide the design of shell-based micromotors.

Experimental Section

Materials and Reagents.

SiO_2 microspheres at different size were obtained from Shanghai Aladdin Bio-Chem Technology Co., Ltd. (China). β-D-Glucose was purchased from Shanghai Macklin Biochemical Co., Ltd. (China). Catalase from bovine liver, GOx from apergillus niger, MUA, MCH, *N*-hydroxycinimide (NHS) and 1-ethyl-3-(3-dimethylaminopropyl) carbodiimide hydrochloride (EDC) were purchased from Sigma–Aldrich. (USA). Ultrapure water used in all experiments was produced from a Millipore water purification system (≥18 MΩ, Milli-Q, Millipore).

Fabrication of Enzyme Powered Microshells.

Firstly, multimetallic microshells were prepared by template-directed deposition. Briefly, SiO_2 microspheres dispersed in ethanol were deposited on glass substrates pretreated by Piranhas acid to form monolayer. After an air drying, Au, Ag and Au were sputtered to templates successively to obtain a multimetallic coat, whose thickness was decided by diameters of microspheres. Afterwards, Janus microspheres were redispersed into washing buffer (PBS, 10 mM, pH 5.5) through a brief ultrasonic treatment. A 3 times washing, the Janus microspheres were further incubated with 1 mM MCH for 8 h to block the outer metal surface. After another washing, 10% hydrofluoric acid was used to etch SiO_2 templates and produce microshells.

The obtained microshells were immersed in the mixture of 1 mM MCH and 25 mM MUA for 8 h to produce MUA monolayer on the concave surface. Next, microshells were mixed with 0.4 M EDC and 0.1 M NHS in PBS for 2 h to activate carboxyl groups of MUA. Finally, with a 2 h incubation in 2 mg mL^{-1} catalase (or the mixture of 2 mg mL^{-1} catalase and 6 mg mL^{-1} GOx), the catalase modified microshells (or the catalase-GOx based bienzyme microshells) were prepared. The enzyme modified microshells were stored at 4 °C in PBS buffer prior to use.

Characterization of the Motion of Microshells.

Before observation, 6 μL microshells was dispersed into 60 μL H_2O_2 or glucose, then 6 μL mixture was casted onto glass slides after a sufficient oscillation. An inverted optical microscope was used to capture motions of microshells. Displacements were obtained by tracking microshells center-to-center. Moreover, mean velocity was calculated based on trajectories and motions were recorded by videos exported from the software of microscope.

Acknowledgements

We gratefully acknowledge the National Natural Science Foundation of China (21575063).

Conflict of interest

The authors declare no conflict of interest.

Keywords: bubble propulsion · enzyme-powered motors · micromotors · microshell · motion mechanism

[1] a) B. Jang, A. Hong, H. E. Kang, C. Alcantara, S. Charreyron, F. Mushtaq, E. Pellicer, R. Buchel, J. Sort, S. S. Lee, B. J. Nelson, S. Pane, *ACS Nano* **2017**, *11*, 6146–6154; b) M. J. Xuan, Z. G. Wu, J. X. Shao, L. R. Dai, T. Y. Si, O. He, *J. Am. Chem. Soc.* **2016**, *138*, 6492–6497; c) D. Zhou, Y. C. Li, P. Xu, N. S. McCool, L. Li, W. Wang, T. E. Mallouk, *Nanoscale* **2017**, *9*, 1315.
[2] T. Li, J. Li, H. Zhang, X. Chang, W. Song, Y. Hu, G. Shao, E. Sandraz, G. Zhang, L. Li, J. Wang, *Small* **2016**, *12*, 6098–6105.
[3] R. Liu, A. Sen, *J. Am. Chem. Soc.* **2011**, *133*, 20064–20067.
[4] T. Xu, F. Soto, W. Gao, R. Dong, V. Garcia-Gradilla, E. Magana, X. Zhang, J. Wang, *J. Am. Chem. Soc.* **2015**, *137*, 2163–2166.

[5] a) B. Esteban-Fernandez de Ávila, P. Angsantikul, J. Li, M. A. Lopez-Ramirez, D. E. Ramirez-Herrera, S. Thamphiwatana, C. Chen, J. Delezuk, R. Samakapiruk, V. Ramez, L. Zhang, J. Wang, *Nat. Commun.* **2017**, *8*, 1299; b) W. Gao, A. Pei, R. Dong, J. Wang, *J. Am. Chem. Soc.* **2014**, *136*, 2276 – 2279.
[6] a) J. Shao, M. Xuan, H. Zhang, X. Lin, Z. Wu, Q. He, *Angew. Chem. Int. Ed.* **2017**, *56*, 12935 – 12939; *Angew. Chem.* **2017**, *129*, 13115 – 13119; b) M. M. Stanton, B.-W. Park, A. Miguel-Lopez, X. Ma, M. Sitti, S. Sanchez, *Small* **2017**, *13*, 1603679.
[7] a) M. Hansen-Bruhn, B. E.-F. de Avila, M. Beltran-Gastelum, J. Zhao, D. E. Ramirez-Herrera, P. Angsantikul, K. V. Gothelf, L. Zhang, J. Wang, *Angew. Chem. Int. Ed.* **2018**, *57*, 2657 – 2661; *Angew. Chem.* **2018**, *130*, 2687 – 2691; b) J. Wu, S. Balasubramanian, D. Kagan, K. M. Manesh, S. Campuzano, J. Wang, *Nat. Commun.* **2010**, *1*, 36.
[8] a) N. Khiem Van, S. D. Minteer, *Chem. Commun.* **2015**, *51*, 4782 – 4784; b) F. Kuralay, S. Sattayasamitsathit, W. Gao, A. Uygun, A. Katzenberg, J. Wang, *J. Am. Chem. Soc.* **2012**, *134*, 15217 – 15220.
[9] a) C. Chen, X. Chang, H. Teymourian, D. E. Ramirez-Herrera, B. Esteban-Fernandez de Ávila, X. Lu, J. Li, S. He, C. Fang, Y. Liang, F. Mou, J. Guan, J. Wang, *Angew. Chem. Int. Ed.* **2018**, *57*, 241 – 245; *Angew. Chem.* **2018**, *130*, 247 – 251; b) W. Gao, X. Feng, A. Pei, Y. Gu, J. Li, J. Wang, *Nanoscale* **2013**, *5*, 4696 – 4700.
[10] a) B. Dai, J. Wang, Z. Xiong, X. Zhan, W. Dai, C.-C. Li, S.-P. Feng, J. Tang, *Nat. Nanotechnol.* **2016**, *11*, 1087 – 1092; b) D. Yi, Q. Zhang, Y. Liu, J. Song, Y. Tang, F. Caruso, Y. Wang, *Angew. Chem. Int. Ed.* **2016**, *55*, 14733 – 14737; *Angew. Chem.* **2016**, *128*, 14953 – 14957.
[11] a) L. Soler, V. Magdanz, V. M. Fomin, S. Sanchez, O. G. Schmidt, *ACS Nano* **2013**, *7*, 9611 – 9620; b) J. Li, V. V. Singh, S. Sattayasamitsathit, J. Orozco, K. Kaufmann, R. Dong, W. Gao, B. Jurado-Sanchez, Y. Fedorak, J. Wang, *ACS Nano* **2014**, *8*, 11118 – 11125.
[12] a) E. Karshalev, R. Kumar, I. Jeerapan, R. Castillo, I. Campos, J. Wang, *Chem. Mater.* **2018**, *30*, 1593 – 1601; b) R. Maria-Hormigos, B. Jurado-Sanchez, A. Escarpa, *Adv. Funct. Mater.* **2018**, *28*, 1704256.
[13] a) S. Fu, X. Zhang, Y. Xie, J. Wu, H. Ju, *Nanoscale* **2017**, *9*, 9026 – 9033; b) Y. Xie, S. Fu, J. Wu, J. Lei, H. Ju, *Biosens. Bioelectron.* **2017**, *87*, 31 – 37.
[14] a) M. Uygun, B. Jurado-Sanchez, D. A. Uygun, V. V. Singh, L. Zhang, J. Wang, *Nanoscale* **2017**, *9*, 18423 – 18429; b) A. C. Hortelão, T. Patino, A. Perez-Jimenez, A. Blanco, S. Sanchez, *Adv. Funct. Mater.* **2018**, *28*, 1705086.
[15] P. Díez, B. E.-F. de Avila, D. E. Ramirez-Herrera, R. Villalonga, J. Wang, *Nanoscale* **2017**, *9*, 14307 – 14311.
[16] J. Orozco, V. Garcia-Gradilla, M. D'Agostino, W. Gao, A. Cortes, J. Wang, *ACS Nano* **2013**, *7*, 818 – 824.
[17] D. Kagan, S. Campuzano, S. Balasubramanian, F. Kuralay, G. U. Flechsig, J. Wang, *Nano Lett.* **2011**, *11*, 2083 – 2087.
[18] M. J. Xuan, X. K. Lin, J. X. Shao, L. R. Dai, Q. He, *ChemPhysChem* **2015**, *16*, 147 – 151.
[19] X. Ma, A. Jannasch, U. R. Albrecht, K. Hahn, A. Miguel-Lopez, E. Schaffer, S. Sanchez, *Nano Lett.* **2015**, *15*, 7043 – 7050.
[20] a) M. Safdar, T. Itkonen, J. Janis, *RSC Adv.* **2015**, *5*, 13171 – 13174; b) Z. Lin, Z. Wu, X. Lin, Q. He, *Chem. Eur. J.* **2016**, *22*, 1587 – 1591.
[21] W. Huang, M. Manjare, Y. Zhao, *J. Phys. Chem. C* **2013**, *117*, 21590 – 21596.
[22] G. Zhao, M. Pumera, *Nanoscale* **2014**, *6*, 11177 – 11180.
[23] W. Z. Teo, H. Wang, M. Pumera, *Chem. Commun.* **2016**, *52*, 4333 – 4336.
[24] a) G. Zhao, M. Pumera, *Phys. Chem. Chem. Phys.* **2012**, *14*, 6456 – 6458; b) Z. Zhang, J. H. Li, L. W. Fu, D. Y. Liu, L. X. Chen, *J. Mater. Chem. A* **2015**, *3*, 7437 – 7444.
[25] X. Ma, S. Jang, M. N. Popescu, W. E. Uspal, A. Miguel-Lopez, K. Hahn, D. P. Kim, S. Sanchez, *ACS Nano* **2016**, *10*, 8751 – 8759.
[26] H. Su, Y. Fang, F. Chen, W. Wang, *Chem. Sci.* **2018**, *9*, 1448 – 1453.
[27] L. L. Wang, L. Chen, J. Zhang, J. M. Duan, L. Wang, Z. H. Silber-Li, X. Zheng, H. H. Cui, *Langmuir* **2018**, *34*, 10426 – 10433.

Manuscript received: March 17, 2019
Revised manuscript received: May 11, 2019
Accepted manuscript online: May 14, 2019
Version of record online: May 27, 2019